Electronic Supplementary Material (ESI) for Energy & Environmental Science.

The role of hydrogen evolution reaction on the solid-electrolyte interphase formation mechanism for "*Water-in-Salt*" electrolytes

Nicolas Dubouis,[a,b] Pierre Lemaire,[a,b,c] Boris Mirvaux,[a,b] Elodie Salager[b,d], Michael Deschamps[b,d], Alexis Grimaud[a,b,c*]

AUTHOR ADDRESS

a) Chimie du Solide et de l'Energie, UMR 8260, Collège de France, 11 Place Marcelin Berthelot, 75231 Paris Cedex 05, France

b) RS2E, Réseau Français sur le Stockage Electrochimique de l'Energie, FR CNRS 3459, F-80039 Amiens Cedex 1, France

c) Sorbonne Universités – UPMC Université Paris 06, Paris, France

d) CNRS, CEMHTI, UPR 3079, Université d'Orléans, Orléans, France

Table of contents

Experimental Details

Materials

All the glassware was rinsed at least 3 times with Milli-Q water prior to use. All chemicals, including lithium bis(trifluoromethanesulfonyl)amide (Solvay), potassium bis(trifluoromethanesulfonyl)amide (99.5%, Solvionic), lithium nitrate (anhydrous, 99%, Alfa Aesar), lithium chloride (anhydrous, 98+%, Alfa Aesar), o-Cresolphtahalein complexone (Alfa Aesar) were used as received from the suppliers, without any purification.

Fourier-Transform Infrared (FTIR) Spectroscopy

FTIR spectra were recorded on a Nicolet iS5 FTIR spectrometer, mounted with a diamond Attenuated Total Reflectance accessory (iD1 ATR). One drop of solution was analyzed using 16 scans with a 4 cm^{-1} resolution from 4,000 to 500 cm^{-1}. Background correction was performed by measuring the ambient atmosphere using the same conditions as for the solution samples.

Nuclear Magnetic Resonance (NMR) Spectroscopy

Liquid-state NMR spectra were recorded on a Bruker 7.046 T Avance III HD NMR spectrometer mounted with a 5 mm HX(F) probehead. For electrolyte analysis, NMR tubes equipped with a D_2O (99% D, Sigma-Aldrich) filled coaxial insert were used in order to lock the magnetic field. Single pulses sequences were used to record ^{1}H, ^{7}Li and ^{19}F spectra for the electrolytes. 90° pulses were optimized for the 1 m LiTFSI solution. As the salinity of the samples may affect the pulses length required for a 90° impulsion, the intensity of the measured signal is not a relevant parameter, therefore intensities were normalized. Experimental parameters used for each nucleus are shown in Table S1.

Nucleus	**^{1}H**	**^{7}Li**	**^{19}F**
Number of scans	16	4	16
Dummy scans	0	4	2
Acquisition time (s)	2	10	5
Recycle time (s)	1	10	10

Table S1. Experimental parameters used in the NMR experiments to characterize the lithium based electrolytes.

For the NMR data shown in Figure 7, a proton decoupled ^{19}F experiment was used with 4 dummy scans, 128 scans, 2 seconds acquisition and 1 second for recycle delay.

Solid-state NMR spectra were recorded on a Bruker 4.7 T Avance III spectrometer mounted with a 1.3 mm double-resonance probehead. Cycled and rinsed gas diffusion layer (two times 30 minutes with DME, and dried under vacuum overnight) was packed into 1.3 mm rotors that were spun at a 50 kHz rate at the magic-angle during data acquisition. Rotor synchronized Hanh-echo sequences were used for the different experiments (^{1}H, ^{7}Li and ^{19}F). Sufficient recycle delays were used to allow a proper quantification (200, 400, and 5 s for ^{1}H, ^{7}Li and ^{19}F respectively). ^{1}H, ^{7}Li and ^{19}F were externally referenced respectively to H_2O in 1 M LiCl (4.70 ppm) 1 M LiCl (0.00 ppm) and fluoroacetophenone at – 107 ppm. Resulting spectra were fitted using DMFIT[1].

Electrochemical measurements

Electrolytes were prepared by precisely weighting a mass of salt and adding the corresponding amount of ultrapure water to obtain the desired molality. Solutions were sonicated for 30 min to ensure a proper dissolution and cooled down to ambient temperature before performing any measurement. Data were acquired either on a Biologic VSP or Biologic VMP3 potentiostats. Ohmic drop was measured using current interrupt technique after the electrochemical measurements. Prior to any measurement, mirror polished glassy carbon (GC) electrodes and platinum electrodes (Pine research) were polished using ultrafine alumina slurries (0.05 µm on microfiber cloth polishing disk for the GC, and three steps for the Pt starting from 5 µm on nylon polishing disk, followed by 0.3 µm and 0.05 µm on microfiber cloth polishing

disk). Residual traces of slurries were removed by sonicating the as polished electrodes in a 50:50 H_2O:EtOH solution two times for 15 minutes. To ensure the cleanliness of platinum electrodes surface, platinum electrodes were hold at + 2.0 V vs. SHE in a 0.5 M H_2SO_4 solution for 2 minutes followed by 10 cycles of cyclic voltammetry (from 1.350 V to 0.0 V vs. SHE) in the same H_2SO_4 solution. Then, freshly cleaned electrodes were rinsed by MQ-water and used within a short time (typically less than 15 minutes).

All electrochemical measurements were recorded using a three electrodes cell setup with a calomel reference electrode (0.240 mV vs. SHE), except for the electrochemical quartz microbalance and the *operando* XRD for which a small $Hg/HgSO_4$ reference electrode (0.685 V vs. SHE) was used. A graphite rod was used as a counter electrode for all measurements. For static measurements, electrodes were immersed in a small volume (typically 2 mL) of solution while larger volume (typically 10 mL) of solutions were used for rotating disk electrode measurements to allow a proper laminar flow of solution on the surface of the rotating electrode. In order to prevent O_2 and CO_2 reduction, electrolytes were degassed (except for *operando* XRD) by bubbling argon (Linde, purity 5.0) for at least 1 hour prior to the first experiment. For static cyclic voltammetry experiments, the cell was closed using septa, and argon flow was stopped during the measurement to avoid convection in the electrolyte.

Ohmic drop was measured using current-interrupt technique after every electrochemical measurement. Typical values from 15 Ω (for 1 molar electrolytes) to 150 Ω (20 m LiTFSI) were measured. The ohmic drop compensation was performed during the data treatment.

On-line electrochemical mass spectrometry

Online gas-analysis was performed using a HIDEN H1 mass spectrometer system (HIDEN Analytical, UK). A 5 necks cell described in Figure M1 was used to perform the electrochemistry. Briefly, the top neck was filled with a plastic cap to avoid dead volume, in which a copper wire was inserted to make the electrical contact with the working electrode. Small necks were used to place a calomel reference electrode, a counter electrode compartment, a gas outlet and a gas inlet. The graphite rod counter electrode was isolated in a glass compartment to avoid O_2 evolution in the electrolyte. The cell was connected to the mass spectrometer through a flexible 1 m capillary inlet and two porous stainless steel membrane filters (~2 µm pore diameter, Valco Instruments Co. Inc.) preventing the capillary for water contamination. A small flow of argon was bubbled through the solution during the measurement to minimize the delay of detection. Electrolytes were degassed during 4 hours before performing the measurement (Ar, O_2, N_2, H_2O, CO_2 and H_2 evolutions were monitored during that time). In order to get more precise values and shorten the acquisition time, only the evolution of H_2 was monitored during the experiment. Shorter experiments (not shown here), confirmed H_2 was the only gas evolved during the electrochemical tests, confirming previous observations by Suo *et al*..[2]

Typical delays were in the range of 1 to 2 minutes, as established by applying a constant negative current in a 1 M H_2SO_4 solution for 10 minutes and monitoring the H_2 evolution. The lowest current for which H_2 evolution was monitored was 1 mA.

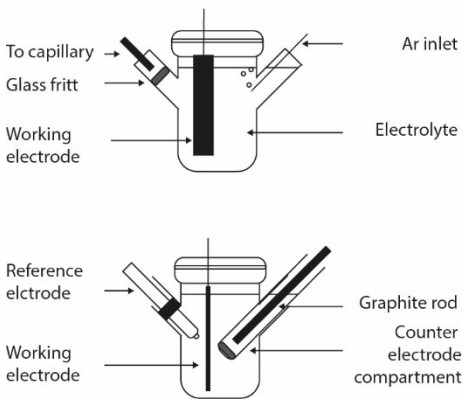

Figure M1. Cell used for the OLEMS measurements (two side views are presented).

Electrochemical Quartz Crystal Microbalance (EQCM)

Electrochemical quartz crystal microbalance (EQCM) measurements were conducted using a commercial SEIKO microbalance (SEIKO QCA 922) with AT-cut 9 MHz quartz covered with carbon on both sides. The electro-active geometric surface area was S = 0.196 cm^2. Simultaneous measurements of the quartz frequency and motional resistance were performed in order to follow both the change in weight of the electrode and the change in viscosity. Motional resistance variations were limited to around 250 Ω during the experiment.

Electrodes characterization

Gas diffusion layer electrodes (Freundenberg H2315/H2) were used to perform the characterization of the electrolyte degradation products as they exhibit a larger surface area than planar glassy carbon electrodes. These electrodes were rinsed and sonicated in ethanol before being used. To ensure the absence of O_2 that can generate Li_2O_2 upon reduction in WiSEs,[3] argon was bubbled during potentiostatic experiments. Finally, in order to remove residual LiTFSI salt before performing *post mortem* characterization, GDL electrodes were washed by soaking them two times for 30 minutes in dimethoxyethane (DME) and dried under vacuum for at least 30 min.

X-ray Diffraction (XRD)

All the diffractograms were acquired on a Bruker D8 advanced diffractometer using a Cu K_α radiation source in a Bragg-Brentano geometry. For *in-situ* measurements, a three electrode cell using a gas diffusion layer working electrode, a graphite counter electrode and a $Hg/HgSO_4$ reference electrode was used, as described in Figure M2.

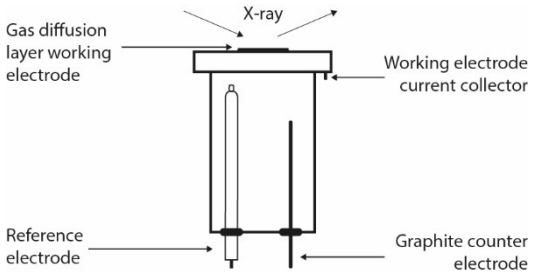

Figure M2. Electrochemical cell used for the *in-situ* XRD characterization.

Scanning Electron Microscopy (SEM) and Energy Dispersive X-ray (EDX)

SEM images were recorded with a SEM-FEG (Hitachi SU-70) and elemental microanalysis with an EDX apparatus (Oxford X_max 50 mm^2), both with a 5 kV acceleration voltage.

Movie and pictures

Pictures for the platinum electrode as well as movies were recorded using a Canon 70D DSLR camera. The speed of the movie presented in the supplementary materials was accelerated by 10 times.

Figures S1 to S6

Figure S1: Nuclear magnetic resonance spectra of saturated LiCl and $LiNO_3$ electrolytes

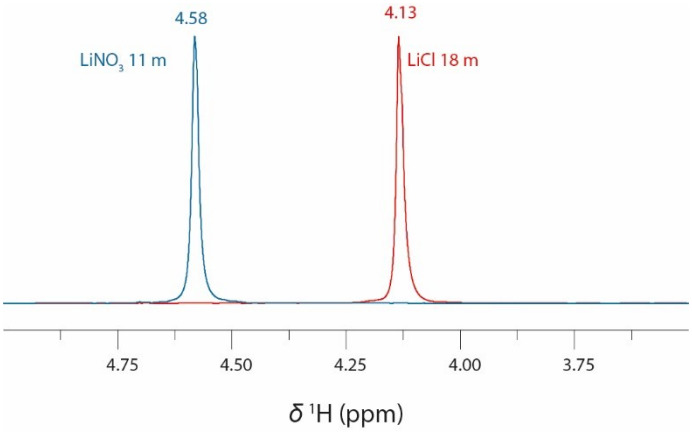

Figure S1. ^1H NMR spectra of aqueous electrolytes containing respectively 11 mol.kg^{-1} of $LiNO_3$ in water (blue) and 18 mol.kg^{-1} of LiCl (red).

Figure S2: Electrochemical Quartz Crystal Microbalance (EQCM)

In order to assess the phenomena responsible for the gain and loss of mass observed by EQCM in Figure 4, we represented the mass gained as a function of the charge to check if the Faraday's law ($m - m_0 = Q\frac{M}{z * F}$ in which z is the number of electrons involved in the reaction) was valid (Figure S2). Since the loss of mass observed during the backward scan did not exhibit any linear region, several electrochemical processes are simultaneously probed. Regarding the forward scans, two linear regions were observed. However, the corresponding molecular weight (calculated for a 1 e$^-$ process) were found to be too low to be consistent with only the electrochemical degradation of TFSI. This observation confirmed the presence of several processes happening simultaneously, some of them leading to a gain of mass as discussed in the main text.

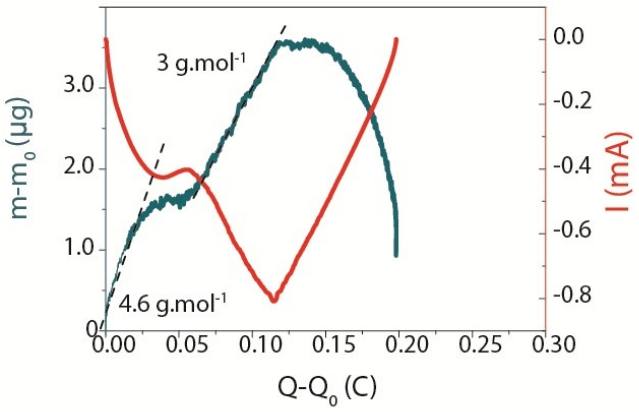

Figure S2. Evolution of the current and the mass monitored on an EQCM electrode in function of the charge passed through the electrode.

Figure S3: Scanning electron microscopy pictures at different magnification of GDL

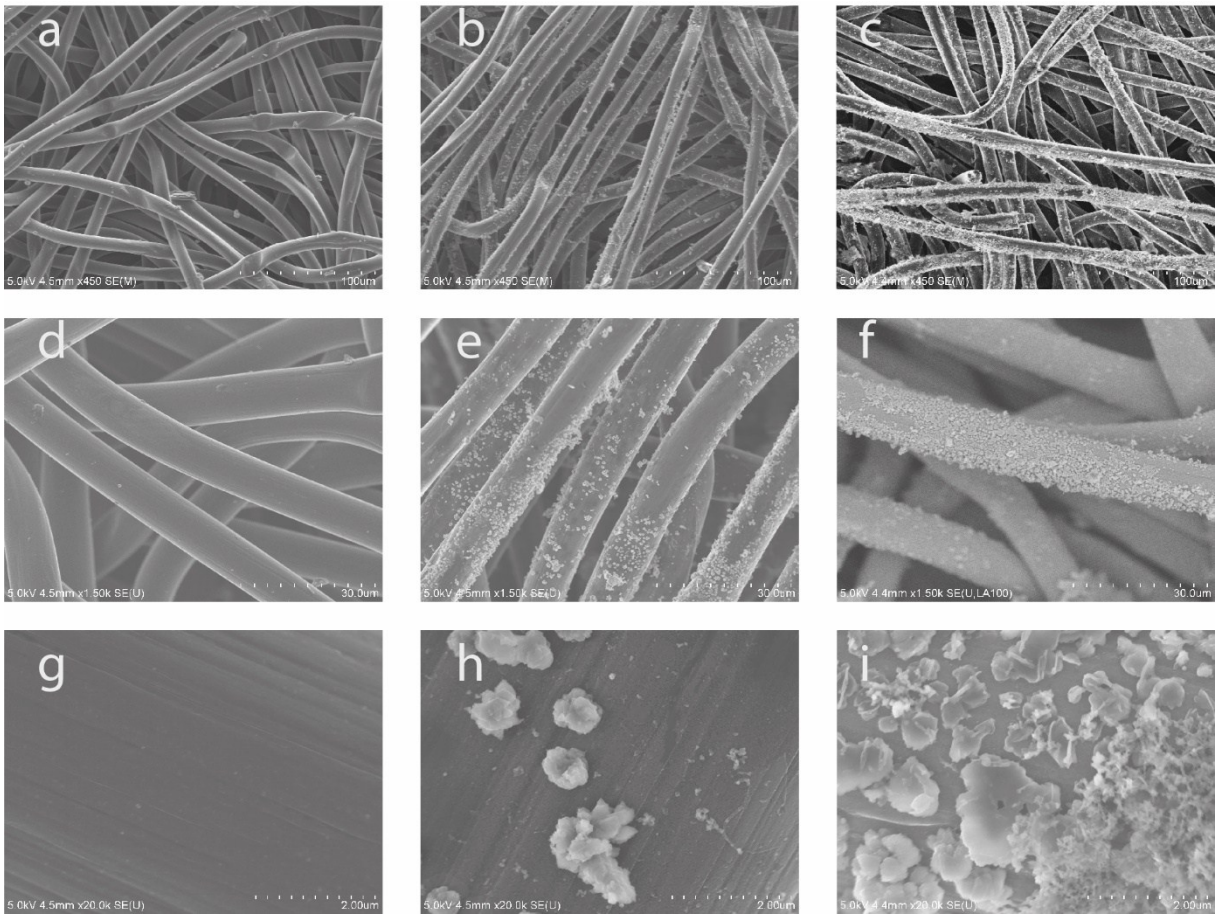

Figure S3. SEM pictures of gas diffusion layer electrodes soaked in 20 m LiTFSI solution (a, d, g), hold at -1.8 V vs. SHE for 3 minutes (b, e, h) and for 10 minutes (c, f, i) at different magnifications (x450, x1,500, x20,000).

Figure S4: Energy dispersive X-ray analysis for cycled GDL electrodes

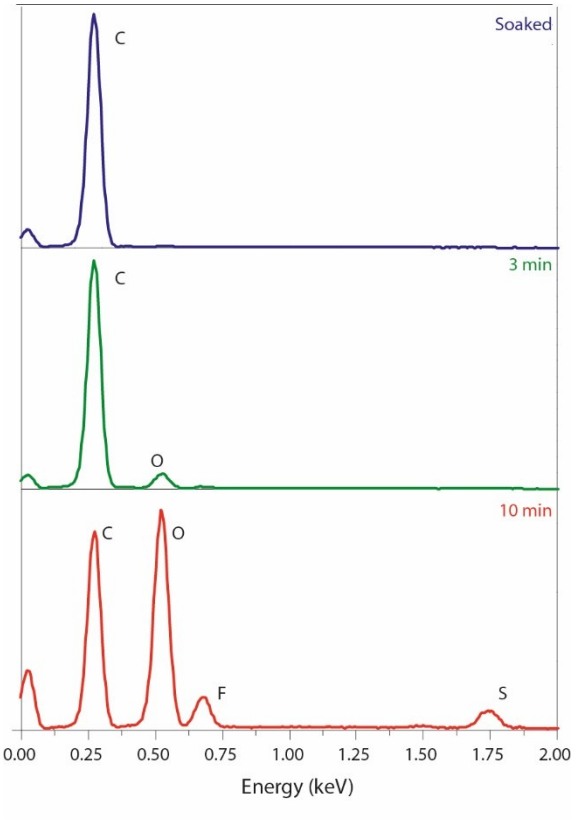

Figure S4. EDX spectra for washed GDL electrodes after being soaked in 20 m LiTFSI (top), hold at -1.8 V vs. SHE for 3 minutes (center) or 10 minutes.

Figure S5: XRD diffractograms recorded between -1.80 and -1.98 V vs. SHE at the end of the *Operando* measurement

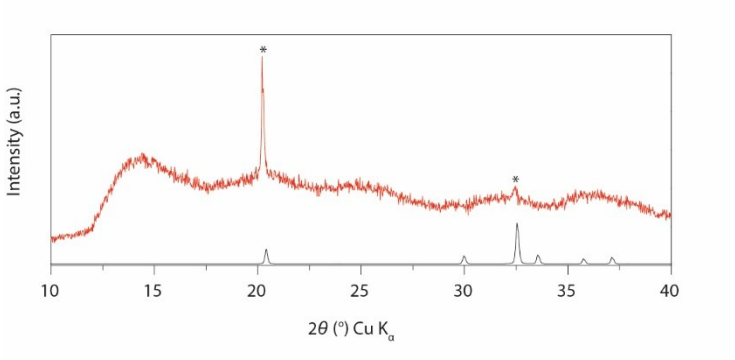

Figure S5. XRD diffractogram of GDL electrode recorded between -1.80 and -1.98 V vs. SHE at the end of the *Operando* measurements shown in Figure 5 (red), and compared with the reference pattern for LiOH (black).[4]

Figure S6: XRD diffractograms for GDL electrodes soaked, soaked an washed, cycled and cycled and washed in 20 m LiTFSI

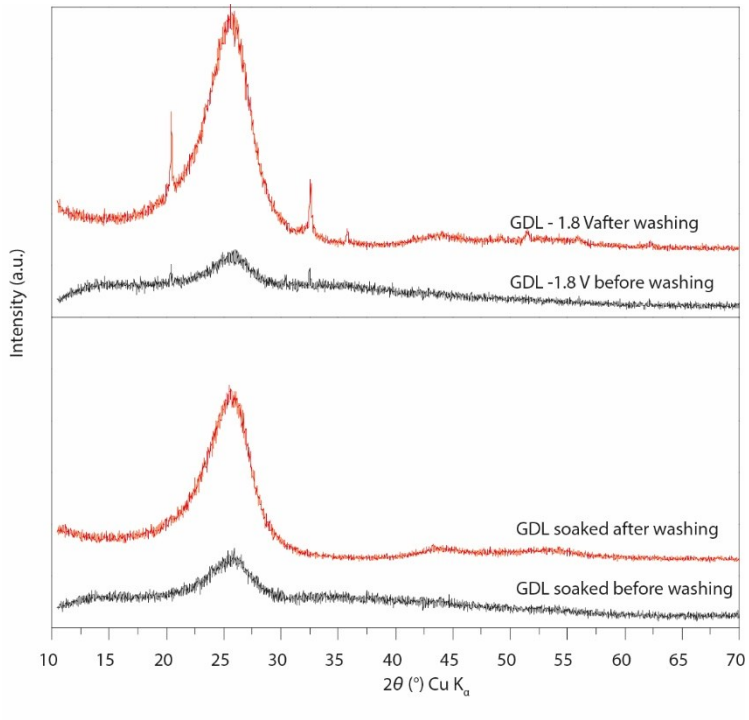

Figure S6. XRD diffractograms collected for GDL electrodes soaked in 20 m LTFSI (bottom) and hold for 10 min at -1.8 V vs. SHE (top) before (black) and after (red) washing with DME.

Figure S7: Additional Solid-state NMR spectra for the Gas Diffusion Layer and reference compounds

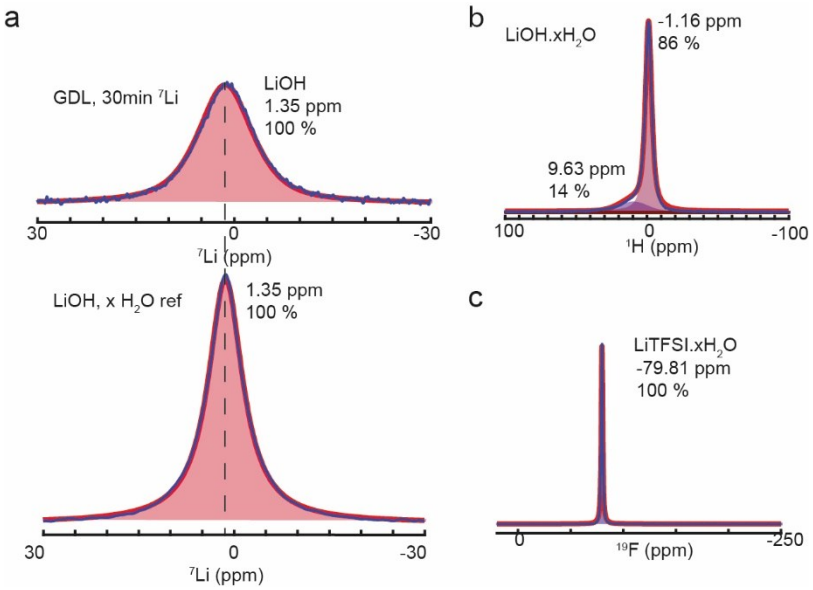

Figure S7. a) ^{7}Li the GDL hold 30 min in 20 mWiSE at -1.8 V vs. SHE (top) compared with hydrated LiOH (bottom), b) ^{1}H MAS NMR spectra of hydrated LiOH and c) ^{19}F MAS NMR spectra of LiTFSI (hydrated).

Figure S7 a) confirms the presence of LiOH in the discharged carbon electrode. Figure S7 b) shows that the presence of a broad signal at around 11 ppm noticed in the main text (Figure 7) for the discharged GDL may arise from some OH groups from residual water situated within crystalline LiOH (around 9.6 ppm in solid LiOH). Figure S7 c) shows the reference ^{19}F signal for LiTFSI $-CF_3$ group.

Discussion on SEI formation by water doping of organic electrolytes (Figure S8)

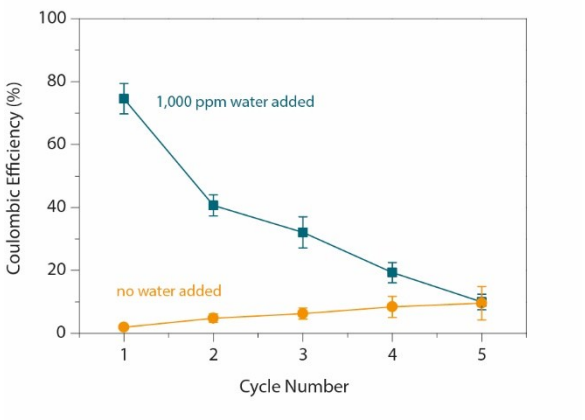

Figure S8. Coulombic efficiency measured during the platting-stripping of lithium (Li) on a copper (Cu) electrode with a 1.0 $mA.cm^{-2}$ current density with LiTFSI (1 M) in DME electrolyte with (blue) or without (orange) 1,000 ppm of water added. The platting/stripping capacity used in the experiment was 0.345 mA.h, similarly to the protocol proposed elsewhere.[5] Li-Cu cells were assembled in an Ar filled glovebox (<0.1 ppm O_2/H_2O), using a coin cell geometry and Cellgard separators.

Having demonstrated that the chemical reaction between hydroxiles ions generated upon water reduction and TFSI anions can trigger the formation of a SEI, we thus decided to investigate the effect of adding small amounts of water in organic electrolytes on the stabilization of the SEI for metallic Li. As shown in Figure S8, adding a small amount of water such as 1,000 ppm drastically increases the initial coulombic efficiency for the Li plating/striping on copper current collector in DME 1 M LiTFSI organic solvent (from less than 5 % to about 80 %). However, after only 5 cycles, the water-rich electrolyte cell behaves the same as the one made with a dry electrolyte. Stabilizing this SEI may be possible by combining different solvents and or salts that present an electrophilic center. Mastering the formation of a stable SEI in organic electrolytes by playing on water reduction products reactivity appears thus as an attractive strategy to the use of high-energy density Li(M) electrodes in organic electrolytes.

Discussion on NMR interpretation

NMR spectra presented in Figure 1 in the main text were normalized. This normalization was performed because the high variation in salt concentration depending on the samples prevents the use of the same pulse length to reach a 90° impulsion. Also, we should emphasize that for a proper interpretation, a correction of those chemical shifts with the magnetic susceptibility should be done. However, the fact that the chemical shift of ^{1}H, ^{7}Li and ^{19}F do not decrease with the same trend (Figure S'1) reveals that other effects such as water-water H-bond breaking, and increase of electronic density due to anionic interactions as described in the main text are responsible for these shifts.

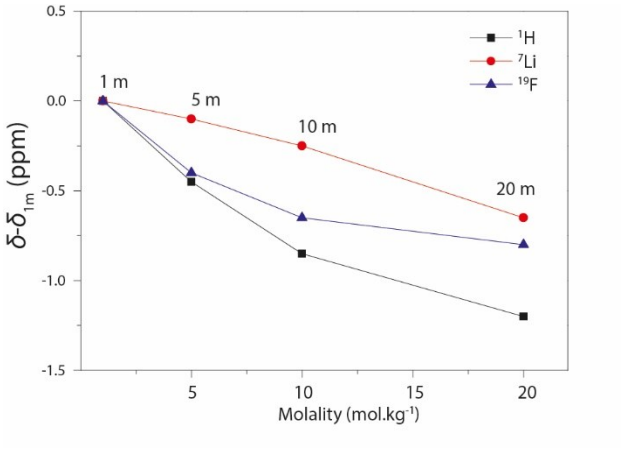

Figure S'1. Evolution of the ^{1}H (squares, black), ^{7}Li (circles, red) and ^{19}F (triangle, blue) chemical shifts of WiSEs depending on the salt molality.

Discussion on platinum electrochemistry

In the main text, on electrochemical results presented in Figure 2, in both static and RDE experiments the presence of a reduction peak before the HER region was found for the platinum electrode. The presence of this peak advocates for the presence of an "underpotential deposited" hydrogen layer (usually referred as the H_{UPD} layer), which is known to influence the catalytic activity of the platinum toward the HER[6]. This phenomenon was previously discussed by Coustan *et al.*[7]

Supporting information references

1 D. Massiot, F. Fayon, M. Capron, I. King, S. L. Calvé, B. Alonso, J.-O. Durand, B. Bujoli, Z. Gan and G. Hoatson, *Magn. Reson. Chem.*, **40**, 70–76.

2 L. Suo, D. Oh, Y. Lin, Z. Zhuo, O. Borodin, T. Gao, F. Wang, A. Kushima, Z. Wang, H.-C. Kim, Y. Qi, W. Yang, F. Pan, J. Li, K. Xu and C. Wang, *J. Am. Chem. Soc.*, 2017, **139**, 18670–18680.

3 Q. Dong, X. Yao, Y. Zhao, M. Qi, X. Zhang, H. Sun, Y. He and D. Wang, *Chem*, , DOI:10.1016/j.chempr.2018.02.015.

4 J. D. Hanawalt, H. W. Rinn and L. K. Frevel, *Ind. Eng. Chem. Anal. Ed.*, 1938, **10**, 457–512.

5 J. L. Goldman, R. M. Mank, J. H. Young and V. R. Koch, *J. Electrochem. Soc.*, 1980, **127**, 1461–1467.

6 I. Ledezma-Yanez, W. D. Z. Wallace, P. Sebastián-Pascual, V. Climent, J. M. Feliu and M. T. M. Koper, *Nat. Energy*, 2017, **2**, 17031.

7 L. Coustan, G. Shul and D. Bélanger, *Electrochem. Commun.*, 2017, **77**, 89–92.